

Photo-responsive droplet manipulation slippery lubricant-infused porous surface with ultra-high durability

Ze-Zhi Liu(刘泽志), Chen Zhang(张琛), Tong Wen(文通), Hui-Zhu Li(李荟竹),Wen-Ping Gao(高文萍), Xin-Kong Wang(王新孔), Wei Zhao(赵伟),Kai-Ge Wang(王凯歌), and Jin-Tao Bai(白晋涛)
Citation: Chin. Phys. B, 2023, 32 (**11**): 116801. DOI: 10.1088/1674-1056/ad0143
Journal homepage: http://cpb.iphy.ac.cn; http://iopscience.iop.org/cpb

What follows is a list of articles you may be interested in

Numerical simulation of two droplets impacting upon a dynamic liquid film

Quan-Yuan Zeng(曾全元), Xiao-Hua Zhang(张小华), and Dao-Bin Ji(纪道斌)
Chin. Phys. B, 2022, 31 (**4**): 046801. DOI: 10.1088/1674-1056/ac22a0

Tolman length of simple droplet: Theoretical study and molecular dynamics simulation

Shu-Wen Cui(崔树稳), Jiu-An Wei(魏久安), Qiang Li(李强), Wei-Wei Liu(刘伟伟), Ping Qian(钱萍), and Xiao Song Wang(王小松)
Chin. Phys. B, 2021, 30 (**1**): 016801. DOI: 10.1088/1674-1056/abb65a

Full filling of mesoporous carbon nanotubes by aqueous solution at room temperature

Xiao-Na Ren(任晓娜), Min Xia(夏敏), Qing-Zhi Yan(燕青芝), Chang-Chun Ge(葛昌纯)
Chin. Phys. B, 2019, 28 (**3**): 036801. DOI: 10.1088/1674-1056/28/3/036801

Approximate expression of Young's equation and molecular dynamics simulation for its applicability

Shu-Wen Cui(崔树稳), Jiu-An Wei(魏久安), Wei-Wei Liu(刘伟伟), Ru-Zeng Zhu(朱如曾), Qian Ping(钱萍)
Chin. Phys. B, 2019, 28 (**1**): 016801. DOI: 10.1088/1674-1056/28/1/016801

Icephobic performance on the aluminum foil-based micro-/nanostructured surface

Yu Chen(陈宇), Guicheng Liu(刘桂成), Lei Jiang(姜磊), Ji Young Kim(金志永), Feng Ye(叶锋), Joong Kee Lee(李重基), Lei Wang(王磊), Bo Wang(王波)
Chin. Phys. B, 2017, 26 (**4**): 046801. DOI: 10.1088/1674-1056/26/4/046801

SPECIAL TOPIC — Celebrating the 100th Anniversary of Physics Discipline of Northwest University

Photo-responsive droplet manipulation slippery lubricant-infused porous surface with ultra-high durability

Ze-Zhi Liu(刘泽志)[1,2,3], Chen Zhang(张琛)[1,2,3,4,†], Tong Wen(文通)[1,2,3], Hui-Zhu Li(李荟竹)[1,2,3], Wen-Ping Gao(高文萍)[1,2,3], Xin-Kong Wang(王新孔)[1,2,3], Wei Zhao(赵伟)[1,2,3], Kai-Ge Wang(王凯歌)[1,2,3,4], and Jin-Tao Bai(白晋涛)[1,2,3,4,‡]

[1] *State Key Laboratory of Photon-Technology in Western China Energy, Xi'an* 710069, *China*
[2] *International Collaborative Center on Photoelectric Technology and Nano Functional Materials, Xi'an* 710069, *China*
[3] *Key Laboratory of Optoelectronics Technology in Shaanxi Province, Xi'an* 710069, *China*
[4] *Institute of Photonics & Photon Technology, Northwest University, Xi'an* 710069, *China*

(Received 1 July 2023; revised manuscript received 4 October 2023; accepted manuscript online 9 October 2023)

Photo-responsive slippery lubricant-infused porous surface (SLIPS) for droplet manipulation is flexible, non-contact and non-destructive in droplet manipulation, which has promising applications in flexible robotics, microfluidics, biomedicine, and chemical analysis. However, the repeated manipulations for droplets of SLIPSs are quite limited in the works reported so far, the poor durability of droplet manipulation severely limits the practical application of the surfaces. In this paper, an Fe_3O_4-doped polydimethylsiloxane (PDMS)-based SLIPS is proposed and implemented to achieve ultra-high repeated droplet manipulation numbers under near-infrared ray (NIR) laser irradiation. Firstly, a micron columnar array structure with micro-pits on the top side, as well as, a wall structure out of the array is designed on SLIPS to reserve the lubricant. Secondly, the prototype of the SLIPS is fabricated by a 3-step ultraviolet (UV) lithography, and subsequently immersed in silicone oil for more than 96 h to obtain the ultra-high durability slippery lubricant-infused porous surface (UD-SLIPS). With a power of 25 mW–85 mW NIR laser, the repeated manipulation of microdroplets ($\leq$ 5 μL) in the scale of 1 cm can exceed more than 3000 times which is far beyond that in previous reports. Finally, the droplet manipulation performance of this photo-responsive UD-SLIPS and the influence of infusion time on durability are investigated. The mechanism of the PDMS swelling effect is found to be the key factor in improving the droplet manipulation durability of SLIPS. The findings of this work would be of great significance for the development of highly durable photo-responsive functional surfaces for droplet manipulation.

Keywords: photo-responsive, droplet manipulation, slippery lubricant-infused porous surface (SLIPS), ultraviolet (UV) lithography

PACS: 68.03.Cd, 81.16.Nd, 68.08.–p, 42.62.–b **DOI:** 10.1088/1674-1056/ad0143

1. Introduction

The functional surfaces for droplet manipulation have been attracting wide-spread attention due to their promising applications in water harvesting,[1–3] self-cleaning,[4–6] anti-icing,[7–9] anti-corrosion,[10–12] and chemical synthesis.[13–15]

The slippery lubricant-infused porous surface (SLIPS) is a commonly typical wettable functional surface, which is usually covered with a lubricant film layer with liquid-repellent capacity, and thus has the characteristics of anti-fouling,[16] anti-compressing,[17] and self-healing.[18] Aizenberg *et al.*[19] proposed to fabricate SLIPS by preparing nanostructures on the epoxy resin surface via replica molding, hydrophobic modifying, and perfluorinated fluids infusing. The correspondingly fabricated SLIPS has an extremely low contact angle hysteresis ($< 2.5°$), low sliding angle ($\leq 5°$), excellent self-healing, pressure stability, and optical transparency. Hao *et al.*[20] prepared an electrowetting on liquid-infused film (EWOLF) by injecting fluorinated liquid or synthetic oils as liquid lubricants into a porous polytetrafluoroethylene (PTFE) film, and locked the lubricant by voltage control of the wetting properties of the liquid and solid phases of the PTFE film to achieve fully reversible wetting properties and suppress droplet oscillation during transient response. By femtosecond laser ablating, Fang *et al.*[21] machined oriented porous microgrooves on an epoxy polymer and followed carbofunctionalized silanes chemical modification, and ferromagnetic fluid injection to obtain a magnetically controllable isotropic/anisotropic lubricated surface. This kind of SLIPS can switch between an isotropic smooth state and an anisotropic grooved state via a magnetic field for directional transportation of liquid droplets. The previously cited studies possess great appeal and immense potential in many areas including drug delivery, liquid robotics, lab-on-a-chip technology, etc. However, the EWOLF asks for a high applied driving voltage and expensive and environmentally harmful lubricants. In addition, the controllable magnetically isotropic/anisotropic SLIPS surfaces are susceptible to external magnetic field interference, and it is difficult to achieve fast, large-area processing based on the femtosec-

[†]Corresponding author. E-mail: nwuzchen@nwu.edu.cn

© 2023 Chinese Physical Society and IOP Publishing Ltd

ond laser ablation.

Photo-responsive slippery surfaces had been considered as promising method for droplet manipulation due to their high precision, non-contact nature, and flexibility.[22] Li *et al.*[23] proposed a paraffin-injected hybrid porous hydroxyapatite nanowire/carbon nanofiber film (PIHPHCF), on which the droplets can be manipulated by controlling the light intensity, surface pattern, and tilt angle. Due to the photothermal effect of carbon nanofiber (CNTs), the paraffin injected into PIHPHCF was changed from a solid state to a liquid state under the irradiation of NIR laser. The viscous force of the surface was much lower as the paraffin was melting; therefore, the droplets could slide on the PIHPHCF. People could control the slide direction of the droplets by adjusting the shape of the NIR laser irradiation region. Qian *et al.*[24] reported a slippery laser-induced graphene/polyimide (SLIG/PI) membrane, in which PI nanofiber membranes were prepared using an electrostatic spinning system, followed by laser carbonization of the surface layer of the PI membrane to construct a porous laser-induced graphene (LIG) structure. The lubricant adopted in the SLIG/PI is silicone oil. With the guidance of NIR laser, the droplets can be transported in any direction and manipulated repeatedly at least 20 times. Huang *et al.*[25] reported a photothermal slippery tube made of MXene-doped PDMS nanosheets, in which heating the substrate with an NIR laser created a wettability gradient that could repeatedly drive droplets at least 20 times in the slippery tube. Photo-responsive SLIPS have developed rapidly in recent years and have shown excellent application prospects in many fields. However, the drawback of poor durability of SLIPS droplet manipulation severely limits the practical application of this type of surface.

In this work, we have designed and implemented a photo-responsive ultra-high durability SLIPS (UD-SLIPS) for droplet manipulation based on the UV lithography. The surface is capable of manipulating microdroplets for more than three thousand times of reciprocal transport which is much higher than that in the so far reported works. The mechanism of obtaining such excellent droplet manipulation capacity has been investigated in detail. The UD-SLIPS can flexibly drive a variety of biochemical droplets, and can also drive droplets against gravity and manipulate droplets for fusion. UD-SLIPS has potential applications in microfluidic chips, cell culture and chemical synthesis.

2. Method

2.1. UV Lithography

In order to obtain ultra-highly durable SLIPS, we proposed to fabricate micron columnar array with micropits on their tops, and wall structures at the periphery of the micron columnar array to improve lubricant locking on the SLIPS surface. In this paper, the 3-step UV lithography method was adopted to the desired structures on the SLIPS.

The fabrication process of the UD-SLIPS is shown in Fig. 1. The first step of the UV lithography is shown in Fig. 1(a), where the photoresist (PR) layer I was formed by spin-coating SU-8 3005 (Kayaku Advanced Materials Inc.,

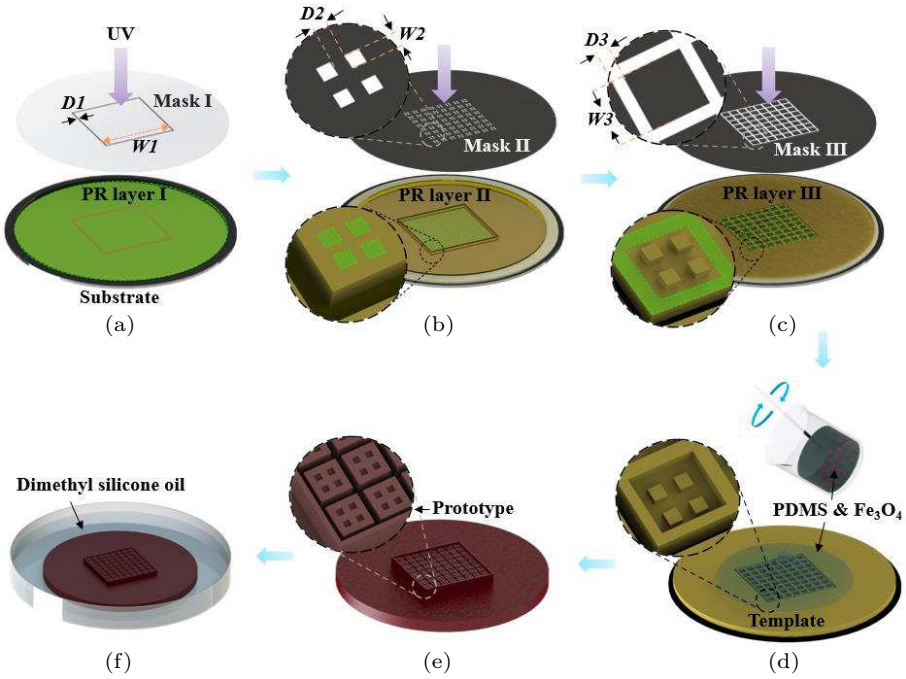


Fig. 1. Preparation of UD-SLIPS via 3-step UV lithography and replica moulding. (a) 1st step: creating a rectangle groove for the replica moulding of the wall structure. (b) 2nd step: creating micro protrusions for the replica moulding of the micropits on SLIPS. (c) 3rd step: creating rectangle wall sides for the replica moulding of the micron columnar array. (d) Replica moulding with Fe_3O_4-doped PDMS. (e) The prototype of SLIPS. (f) Complete the SLIPS by infusing lubricant into the prototype.

Westborough, MA, USA) on the silicon wafer (thickness is about 70 μm), and the rectangle border pattern was imprinted on layer I by using the mask I. The pattern will become the replica moulding of the wall structure after subsequent development. The wall is square-shaped with a side length of $W1 = 1.3$ cm and width $D1 = 100$ μm. Since SU-8 is negative-tone photoresist, the pattern of mask I is non-transparent, and the exposure area is shown in green in Fig. 1(a). The intensity parameter of the UV lithography system is 5 mW/cm^2, 9 times intermittent exposure with 2 s lasting time and 8 s intervals is adopted in the lithography. After exposure, the sample is baked at 95 °C for 10 min to accelerate the curing reaction of SU-8, and then the sample is developed for 2 min, and the first stage lithography is completed by baking the mold at 160 °C for 3 h. The fabrication results are shown in the illustration in the lower left of Fig. 1(b).

The second step of the UV lithography is shown in Fig. 1(b), where the PR layer II was spin-coated (SU-8 3035, Kayaku Advanced Materials Inc., USA) with a thickness of about 5 μm on the structure obtained by the first step. Then, UV light with an intensity of 5 mW/cm^2 is adopted in the exposures (intermittent exposure for 8 times, 2 s per exposure with an 8 s interval). Then the pattern of mask II is transferred to PR layer II to form micron bumps. The square pattern on mask II is transparent with a side length of $W2 = 20$ μm and a spacing between patterns of $D2 = 20$ μm. The same parameters of baking, developing, and curing in the first step are adopted, and the fabrication result is shown in the lower left in Fig. 1(c).

The third step of UV lithography is shown in Fig. 1(c), where SU-8 3005 (PR layer III) with a thickness of about 70 μm was spin-coated on the structure formed by the last step. Then, 12 intermittent exposures (1 s per exposure and 9 s per interval) with a UV light intensity of 5 mW/cm^2 were used to transfer the pattern of mask III to PR layer III to create the sidewalls for the subsequent micron column moulding. The square pattern on mask III was non-transparent, with side length $W3 = 80$ μm and pitch $D3 = 15$ μm. The same baking, developing, and curing steps as in the previous steps were adopted. The resulting structure is shown in the enlarged figure in Fig. 1(d).

2.2. Replica moulding and infusion

Fe_3O_4 nanoparticles (diameter of 20 nm, Shanghai Macklin Biochemical Co., Ltd., Shanghai, China) with strong photothermal effect in the near-infrared wavelength band were selected as the photothermal material in the experiment. Due to the hydrophilic nature of Fe_3O_4 nanoparticles, they needed to be modified into hydrophobic particles before being doped into PDMS: (i) Fe_3O_4 nanoparticles were placed in 3-(trimethoxysilyl) propyl methacrylate (KH570, Shanghai Yuanye Bio-Technology Co., Ltd., China) and stirred for 1 h. The particles were extracted by centrifugation technique and heated at 45 °C for 6 h to remove the solvent. (ii) By mechanical stirring for 2 h, the treated Fe_3O_4 nanoparticles were dispersed (5% by weight) in the PDMS prepolymer (Momentive Performance Materials Inc., USA). (iii) The hardener (10:1 ratio with the prepolymer) was added to the mixture and stirred for 10 min to obtain the photothermal colloid.

As shown in Fig. 1(d), the prepared photothermal colloid was poured onto the template, and the sample was evacuated for 2 h to remove air bubbles. Then, the colloid was cured at 80 °C for 1 h and peeled off from the template to obtain the UD-SLIPS prototype (as shown in Fig. 1(e)). Finally, the UD-SLIPS prototype was immersed in the 5cSt dimethyl silicone oil (Rhone Poulenc Corporation, France) for 96 h, as shown in Fig. 1(f), and then the UD-SLIPS was placed upright for 5 min to remove the excessive lubricant on the surface.

Contact angle measurement (DSA100B, KRÜSS Scientific Instruments, Inc., Germany), high-speed camera (FASTCAM Mini UX100, Photron Limited, Japan) and complementary metal oxide semiconductor camera (CMOS, MER-2000-19U3M/C-L. China Daheng Group, Inc., China) were used to observe the droplet manipulation of the SLIPS. The internal and external structures of the samples were characterized by scanning electron microscope (SEM, Apreo S, Thermo Fisher Scientific Inc., USA). An NIR laser (HW808AD300-16GD, Shenzhen Infrared Laser Technology Co., Ltd., China) with a center wavelength of 808 nm and a beam waist of 1.4 mm^2 was used to manipulate the droplets.

3. Results

3.1. UD-SLIPS processing results

Figure 2(a) shows the SEM characterization of the surface morphology of the SLIPS. It can be seen that the height of the constructed wall ($H1$) is about 140 μm basically equal to the total thickness of the PR layer I and PR layer III. The width of the wall is about 100 μm basically equal to $D1$ in the mask I. The height of the micron column ($H2$) is about 70 μm basically equal to the thickness of the PR layer III. Meanwhile, the edge length of the micron column is about 80 μm and the spacing is about 15 μm, which correspond to $W3$ and $D3$ in masks II and III, respectively. The top surface of the micron column is modified with micropit structures to improve the reservation of lubricant. The depth of the micropit consists of the thickness of the PR layer II (5 μm), and the side length and spacing of the micropit correspond to $W2$ and $D2$ of the mask II. The above results show that the 3-step UV lithography technique used in this paper successfully constructed the designed microstructures on the SLIPS.

Figure 2(b) shows the changes in contact angle (CA) and sliding angle (SA) of droplets on the surface before and after

silicone oil infusion. The CA of the surface before silicone oil infusion can reach 145°, and the droplet (5 μL) can be pinned to the surface when the surface is vertically placed (SA of 90°). The CA of the surface after silicone oil infusion decreases to 91°, the SA of the surface is only 3°, and the adhesion of surface has changed from high to low.

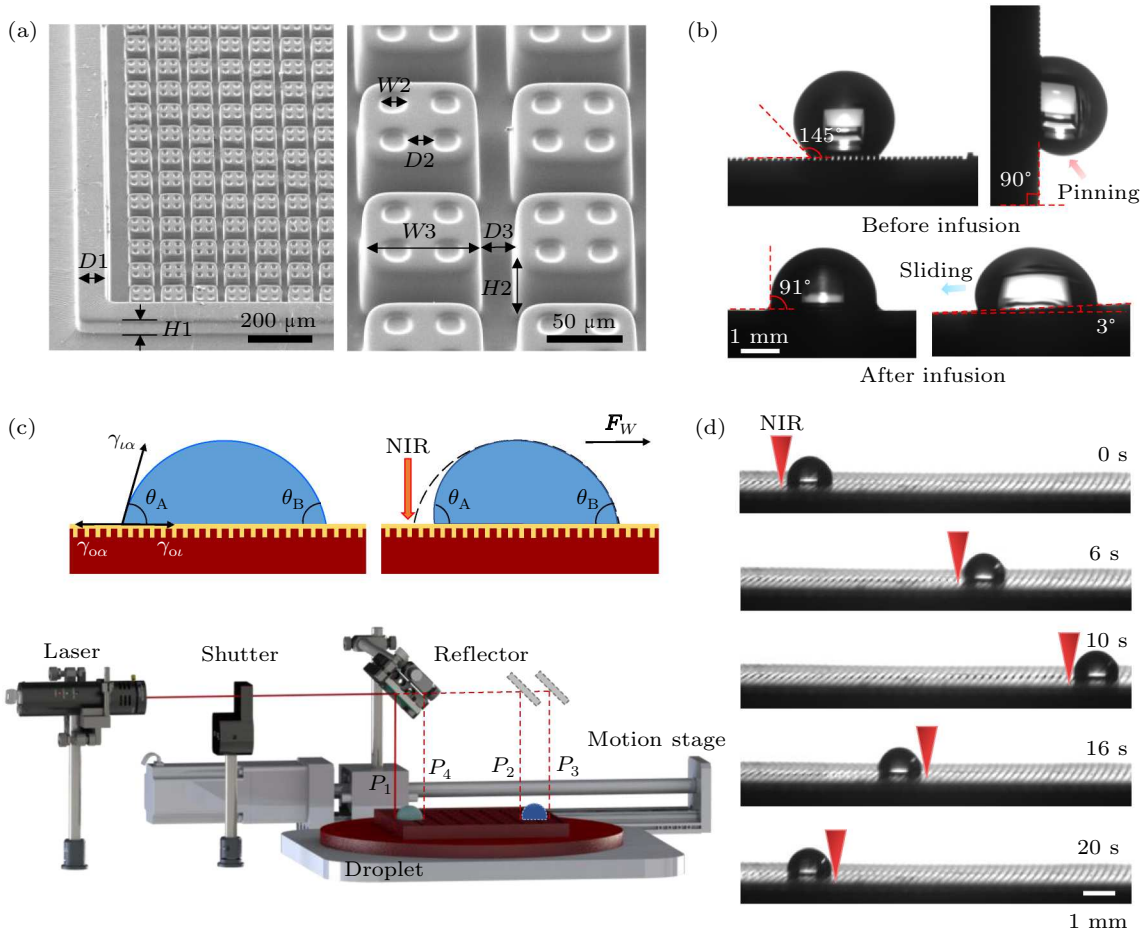


Fig. 2. UD-SLIPS fabrication results and droplet manipulation experiments. (a) SEM characterization of the UD-SLIPS surface morphology. (b) Comparison of contact and sliding angles before and after lubricant infusion. (c) Principle and setup diagram of the droplet manipulation experiments. (d) Droplet reciprocal transport on the UD-SLIPS by NIR laser.

Figure 2(c) shows the droplet manipulation principle and the experimental device. In the figure, $\gamma_{o\alpha}$, $\gamma_{o\iota}$ and $\gamma_{\iota\alpha}$ are the stresses at the oil-gas, oil-liquid, and liquid-gas interfaces, respectively. In the absence of NIR laser irradiation, the droplets are in equilibrium because the forward contact angle θ_A and the backward contact angle θ_B of the droplets are equal. When the light irradiated the droplet side of the surface, the temperature of the SLIPS would be increased and the surface tension of silicone oil would be decreased simultaneously. According to the classical Young's equation[26] $\cos\theta = (\gamma_{o\alpha} - \gamma_{o\iota})/\gamma_{\iota\alpha}$, the droplet advance contact angle θ_A will increase, thus the equilibrium of the original contact angle of the droplet will be broken, which generates the wetting gradient force ($\boldsymbol{F}_W$) upon the droplet[27]

$$\boldsymbol{F}_W \approx 2R(\cos\theta_B - \cos\theta_A)\gamma_{\iota\alpha}, \tag{1}$$

where R is the length of the radius of the contact surface between the droplet and the substrate.

Figure 2(c) also shows the experimental droplet manipulation experimental setup built to manipulate the droplets on SLIPS repeatedly. A motion stage was applied to control the position of a reflector, and a mechanical shutter was used to control the light on and off. In the droplet manipulation, the NIR laser was turned on when the reflector was moved to P_1 and turned off at P_2. Then, the light was turned on at P_3, turned off at P_4, turned on again at P_1 and so on to manipulate the droplet in cycles. The process of a 2 μL droplet driven by NIR laser on SLIPS was captured by the contact angle measuring instrument and shown in Fig. 2(d). The speed of the driving droplet could reach 0.93 mm/s at an NIR laser power of 85 mW.

3.2. UD-SLIPS performance

The performance of the SLIPS in manipulating droplets is influenced by many factors, including laser power, droplet volume, and lubricant infusion time. SLIPS infused with 5cSt dimethyl silicone oil for 24 h are applied in Figs. 3(a)–3(d). Figure 3(a) shows the time evolution of the center temperature

distribution and surface tension of the SLIPS under 85 mW laser irradiation. It can be seen that the surface temperature of the SLIPS increased rapidly from 27.1 °C to 99.5 °C within 1 s. After the NIR laser is turned off, the temperature decreases slowly to 48.6 °C within 3 s. In addition, the relationship between temperature changes and surface tension of silicone oil was studied by Ricci *et al.*[28]

$$\sigma = 20.23 - 6.48 \times 10^{-2} T, \tag{2}$$

where σ represents the surface tension of the silicone oil, T is the surface temperature.

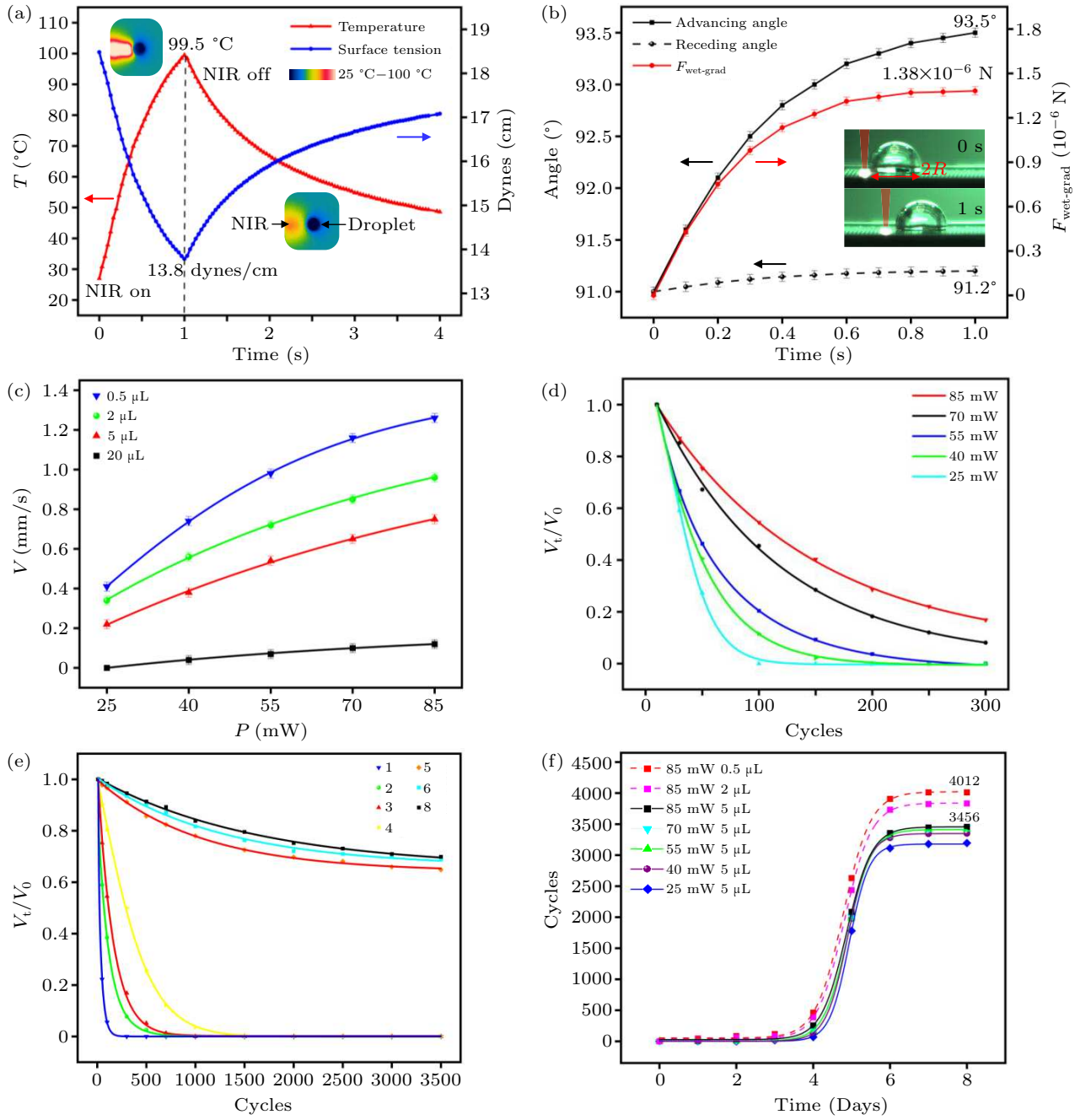


Fig. 3. SLIPS performance with different parameters. SLIPS infused by the 5cSt dimethyl silicone oil for 24 h (a) the variation of temperature and oil–gas tension under 85 mW NIR laser irradiation, (b) the variation of advancing and receding contact angle and wetting gradient force under 85 mW NIR laser irradiation, (c) the variation of droplet transport speed with different laser powers and droplet volumes, (d) the variation of droplet transport speed in different repeated manipulation cycles. SLIPS with different infusion times (e) variation of the droplet transportation speed in different repeated manipulation cycles, (f) variation of the repeated manipulation cycle numbers.

Figure 3(b) shows the variation of the advancing and receding contact angles and the wetting gradient force of droplets on SLIPS along with time under 85 mW laser irradiation. The advancing contact angle θ_A on the left side of the droplet and the receding contact angle θ_B on the right side of the droplet increase from 91°/91° to 93.5°/91.2°, respectively. Meanwhile, since the radius length R of the contact area between the droplet and the substrate remains almost constant

at 0.13 mm, it follows from formula (1) that the wetting gradient force ($\boldsymbol{F}_{\mathrm{W}}$) of the droplet on SLIPS ranges from 0 to 1.38 $\times 10^{-6}$ N during 1 s of light irradiation. The variations of the droplet motion speed with laser power and droplet volume are then investigated.

Figure 3(c) shows the motion speed of droplets with different droplet volumes at different laser powers. The smaller the droplet volume and the higher the laser power is, the faster the droplet moves. The speed of a 0.5 μL droplet can reach 1.26 mm/s under 85 mW laser irradiation. Figure 3(d) shows the ratio of the motion speed V_{t} to the initial speed V_0 of a 5 μL droplet reciprocating over a range of 1 cm under different laser powers (for simplicity, the length of the repeated manipulation of the droplet is configured to 1 cm through the whole investigation). It is found that the droplet motion speed gradually decreased with increasing cycle numbers at different powers. However, the decrease of speed is slower at the higher power than that at the lower power.

As shown in Fig. 3(e), as the SLIPS infused with different time and the power of the NIR laser is 85 mW, the ratio of 5 μL droplet motion speed V_{t} to initial speed V_0 varies with droplet manipulation cycle numbers. The study find that for the same number of the repeated manipulation cycles, the droplet motion speed on the SLIPS decreases slower with a longer infusion time SLIPS, e.g., in the 500th cycle, the ratios of motion speed V_{t} to initial speed V_0 of the SLIPSs infused from 1 day to 7 days are 0, 0.03, 0.05, 0.26, 0.86, 0.90, and 0.91, respectively. The trend of droplet motion speed decrease is slowed down obviously as the infusion time is increased, which indicates that the infusion time improves the durability of SLIPS.

Figure 3(f) shows the effective droplet manipulation cycle numbers of different volumes under different NIR laser powers as the infusion time of SLIPS is increased. For simplicity, the effective repeated manipulation cycle number only considers the cycles in which the speed of the droplet exceeds 70% of the initial speed V_0. It can be seen that with a longer infusion time, smaller droplet volume, and higher laser power, the effective repeated manipulation cycle number would get a higher score. Compared to droplet volume and laser power, infusion time plays a critical role in increasing the effective repeated manipulation cycle number. When the SLIPS is infused with silicone oil for 7 days, the effective repeated manipulation cycle number is up to 3400 for 5 μL droplets, 3800 for 2 μL droplets, and 4000 for 0.5 μL droplets at 85 mW NIR laser power, which could be named as UD-SLIPS.

In the most recent research of the droplet manipulation utilizing photo-responsive SLIPS, Wu *et al.*[29] achieved more than 50 times droplet repeated manipulating with near-infrared laser based on an Fe_3O_4-doped PDMS SLIPS processed by femtosecond laser. Huang *et al.*[25] reported approximately 20 times reciprocal transportation of droplets using the MXene-based photothermal slippery tubes. In our previous study,[22] we were able to enhance the repeated manipulation of droplets over 600 times by modifying the surface structure of SLIPS with polyvinylpyrrolidone particles. In this work, the repeated manipulation of droplets had exceeded 3000 times, which reveals an excellent performance of UD-SLIPS in the droplet manipulations compared with so far reported representative works.

4. Discussion

4.1. Mechanism of UD-SLIPS in droplet manipulation

Figure 4 shows the volume and mass of the SLIPS as a function of lubricant infusion time. Figure 4(a) shows that the volume of the UD-SLIPS before lubricant infusion is 1265 mm^3 and the mass is 1.41 g, while after 7 days of lubricant infusion, the volume and mass increased to 2347 mm^3 and 2.42 g, respectively. Figure 4(b) shows that the volume of UD-SLIPS increases with increasing lubricant infusion time, but the volume does not change significantly after the fourth day. We have tested four groups of UD-SLIPS with different initial volumes and masses. Figure 4(c) shows that the mass of UD-SLIPS also increases with increasing lubricant infusion time and tends to stabilize around the fourth day. The change in volume and mass of SLIPS is due to the swelling of the PDMS substrate during the silicone oil infiltration process. The swelling is levelled off after the fourth day, and the volume and mass of SLIPS do not increase significantly.

Figure 5 shows the principle of how the UD-SLIPS achieves ultra-high durability photo-responsive droplet manipulation. The swelling effect is a physical process as shown in Fig. 5(a).[30] The mixing of dimethyl silicone oil solvent molecules with PDMS polymer chains causes the structure of the polymer chains to change from highly random coiling to partial stretching. At the macroscopic level, the mixing of dimethyl silicone oil solvent molecules with PDMS polymer chains results in an increase in the mass of the composite material, while the change in the structure of the polymer chains from highly random coiling to partial stretching results in an increase in the volume of the composite material. Figure 5(b) shows the cross-sectional SEM images of the UD-SLIPS for two and seven days of silicone oil infusion, respectively, from which it can be clearly observed that the micropores in UD-SLIPS become larger as the silicone oil infusion time increases. This phenomenon further confirms the swelling of the UD-SLIPS in dimethyl silicone oil. The swelling effect allows SLIPS to trap more layers of lubricant, which contributes to increased operating life of functional surfaces.

The swelling of the SLIPS reaches saturation around the 4th day, as shown in Fig. 4. At this point, the dimethyl silicone oil is no longer covalently bound to the PDMS matrix,

but is physically mixed into the cross-linked polymer network. Actually, the PDMS polymer chains are swollen by dimethyl silicone oil to lead to strong interactions between them. Meanwhile, the short molecular chains of dimethyl silicone oil can be anchored by the cross-linked network formed by the PDMS polymer chains to prevent significant silicone oil exudation in a short period of time.[30] However, some of the dimethyl silicone oil will permeate out of the SLIPS under NIR laser cycling irradiation, as shown in Fig. 5(c). On the one hand, the thermal expansion of the PDMS and the increased thermal movement of the silicone oil after the temperature of the laser irradiation area increases cause the silicone oil to permeate out of the PDMS layer. On the other hand, the higher temperature silicone oil region will move toward the lower temperature silicone oil region, thus extracting the silicone oil from the PDMS and permeating it to the surface.

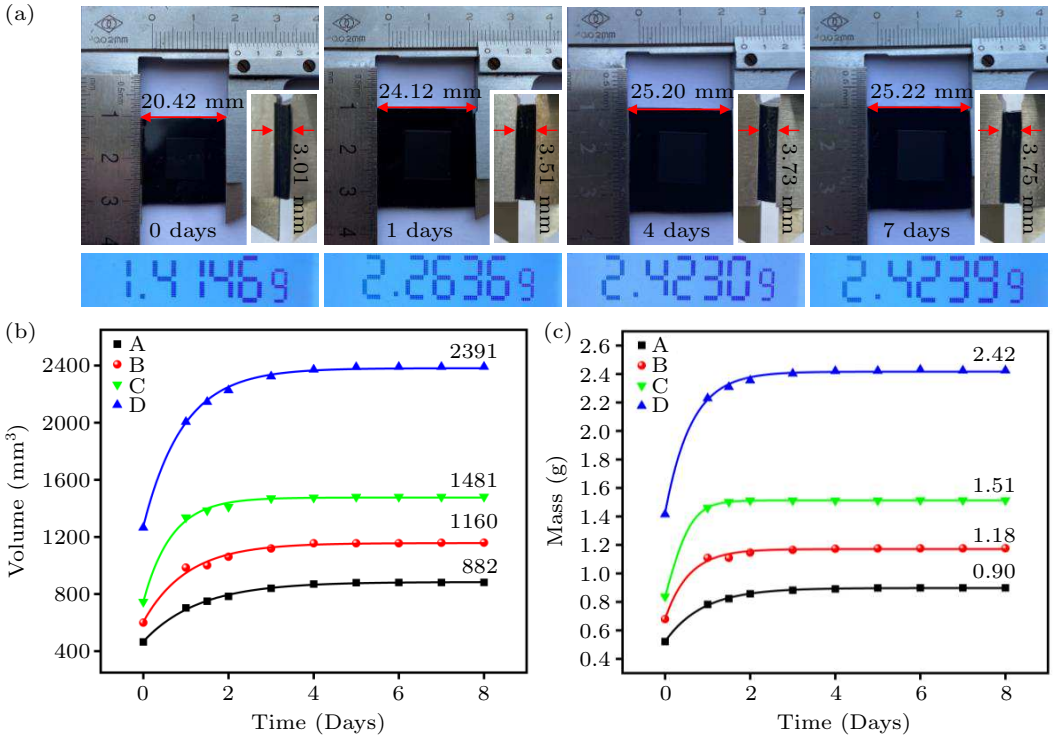


Fig. 4. The variation of volume and mass of the SLIPS with different infusion time. (a) The change of SLIPS in volume and mass. (b) Volume and (c) mass as a function of infusion time.

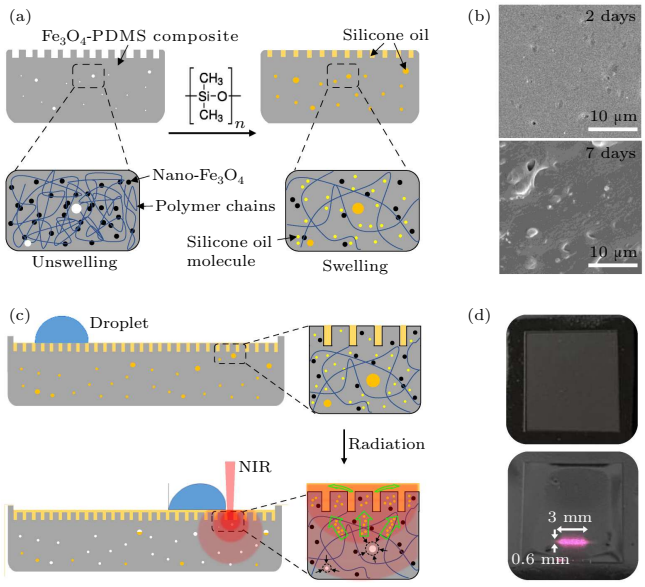


Fig. 5. Ultra-high durability photo-responsive droplet manipulation mechanism of the UD-SLIPS. (a) Schematic diagram of the swelling effect. (b) SEM images of the cross-section of the UD-SLIPS before and after swelling. (c) Mechanism of the silicone oil movement during NIR laser manipulation. (d) Photograph of the UD-SLIPS after long-time use.

The importance of the silicone oil layer in driving the droplets was confirmed in the report by Wen *et al.*[22] After the droplets have been driven several times, the Marangoni effect (ME) causes the local silicone oil layer to be gradually pushed away by the laser spot,[31] leading to a gradual decrease in the driving speed of the droplets, as shown in the first four days of Fig. 3(e). However, in UD-SLIPS, after the saturation of the swelling effect, the composite continuously penetrates the silicone oil under cyclic NIR laser irradiation. Meanwhile, the microcolumn structure and the outermost wall structure on the surface of UD-SLIPS are conducive to the preservation of silicone oil, which ensures that the surface silicone oil layer is sufficiently replenished. As a result, the effective repeated manipulation cycle number of the droplets increases rapidly after soaking for four days.

Figure 5(d) shows the situation of the UD-SLIPS of silicone oil infusion for seven days after long-term NIR laser irradiation. No dimethyl silicone oil exudation was observed in UD-SLIPS without NIR laser irradiation, while UD-SLIPS after 6 h of NIR laser cycling irradiation showed clear exu-

dation of dimethyl silicone oil. The exuded dimethyl silicone oil re-infiltrated the SLIPS after 24 h, and the durability of the UD-SLIPS did not show any significant decrease, indicating that the surface of this type of photo-responsive droplet manipulation has good self-repair capability.

4.2. Application of UD-SLIPS

Figure 6 illustrates the control versatility of the UD-SLIPS. Besides the pure water, UD-SLIPS can also manipulate droplets of biochemical reagents. Figure 6(a) shows the manipulation of six different reagent droplets (I)–(VI), including HepG2 cell fluid (I), milk (II), NaCl solution (III), blood (IV), 50 vol% ethanol (V), and 50 vol% IPA (VI). The volume of the droplets is 2 μL for simplicity. Meanwhile, the effective repeated manipulation cycle number of all reagent droplets is measured at 85 mW laser power. The effective repeated manipulation cycle number of the I–VI reagent droplets is basically similar to that of the water droplets, as shown in Fig. 6(b).

Droplet fusion and inverse gravity transport can be achieved on the UD-SLIPS. In the left panel of Fig. 6(c), 2 μL of 50 vol% ethanol is driven to fusion with pure water by a laser power of 85 mW. In the right illustration of Fig. 6(c), an 85 mW laser can drive a droplet from the bottom to the top of the UD-SLIPS tilted at 8° with a transmission rate of 0.6 mm/s.

The bubbles on UD-SLIPS can also be controlled with high flexibility and diversity by NIR laser irradiation when UD-SLIPS is placed under water. As shown in Fig. 6(d), when an 85 mW NIR laser is used to irradiate submerged UD-SLIPS, the laser spots pull the bubbles on UD-SLIPS to move and further promote their fusion. The driving mode is different from driving droplets in the air.

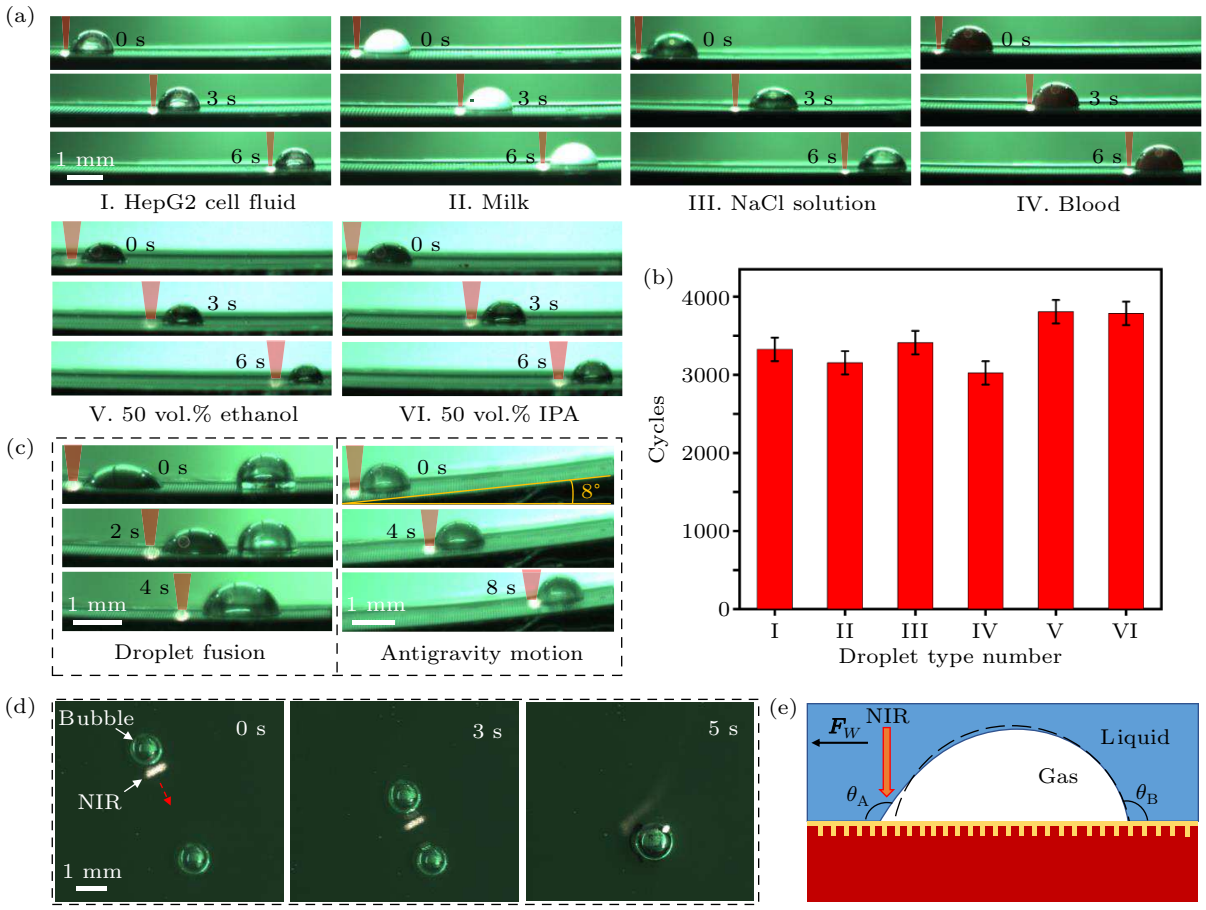


Fig. 6. The UD-SLIPS application scenario. (a) Manipulation of the motion of different droplet types. (b) Effective repeated manipulation cycle number of different droplet types. (c) Manipulation of droplet fusion and inverse gravity transport. (d) Manipulating underwater bubble coalescence. (e) The schematic diagram of underwater bubble traction.

Although the manipulation mode for bubbles on submerged UD-SLIPS and droplets on UD-SLIPS in air are different, their driving principles are similar. In Fig. 6(e), the bubble remains stable on the UD-SLIPS without NIR laser irradiation because the contact angles on both sides of the bubble are equal and there is no wetting gradient force. When the NIR laser excites one side of the bubble, the temperature will be increased in the irradiated area, which causes the surface tension of the silicone oil to decrease. In addition, according to the above Young's equation, the advancing contact angle θ_A of the bubble will be increased as the temperature increases, which results in the irregular asymmetric deformation. An asymmet-

ric wetting gradient force which is generated for the bubble will be spontaneously restored to its original shape. Since the irregular asymmetric deformation of the bubble is opposite to that of the droplet, it results in opposite asymmetric wetting gradient forces. This manifests itself in experimental observations as pushing of the droplet in air and pulling of the bubble in water.

5. Conclusion

An ultra-high durability photo-responsive SLIPS based on the Fe_3O_4 doping is designed by 3-step UV lithography. The UD-SLIPS is capable to perform over three thousand repeated manipulations of 0.5 μL–5 μL sized droplets under 25 mW–85 mW NIR laser irradiation. This is much higher than reported in the previous reports. In addition, the effects of laser power, droplet volume, and lubricant infusion time on the droplet transfer speed are thoroughly investigated. It is shown that the swelling effect contributes to the increased durability of UD-SLIPS. And the mechanism of microscopic movement of lubricant during manipulation of droplets by UD-SLIPS is explained. In addition, the application of UD-SLIPS in various types of droplets and bubble manipulation is demonstrated.

Acknowledgments

Project supported by the National Major Scientific Research Instrument Development Project of China (Grant No. 51927804), the National Natural Science Foundation of China (Grant No. 62275216), and the Science and Technology Innovation Team Project of Shaanxi Province (Grant Nos. S2018-ZC-TD-0061 and 2023-CX-TD-06).

References

[1] Feng R, Xu C, Song F, Wang F, Wang X L and Wang Y Z 2020 *ACS Appl. Mater. Interfaces* **12** 12373
[2] Wier K A and McCarthy T J 2006 *Langmuir* **22** 2433
[3] Gou X and Guo Z 2020 *Langmuir* **36** 8983
[4] Saini A, Arora I and Ratan J K 2020 *Mater. Lett.* **260** 126888
[5] Li X, Yin S, Huang S, Luo H and Tang Q 2020 *Vacuum* **173** 109172
[6] Maharjan S, Liao K S, Wang A J, Barton K, Haldar A, Alley N J, Byrne H J and Curran S A 2020 *Mater. Chem. Phys.* **239** 122000
[7] Ruan M, Zhan Y, Wu Y, Wang X, Li W, Chen Y, Wei M, Wang X and Deng X 2017 *RSC Adv.* **7** 41339
[8] Barthwal S, Lee B and Lim S H 2019 *Appl. Surf. Sci.* **496** 143677
[9] Liu C, Li Y, Lu C, Liu Y, Feng S and Liu Y 2020 *ACS Appl. Mater. Interfaces* **12** 25471
[10] Zhang M, Liu Q, Chen R, Chen H, Song D, Liu J, Zhang H, Li R, Wang Y and Wang J 2018 *J. Alloys Compd.* **764** 730
[11] Song F, Wu C, Chen H, Liu Q, Liu J, Chen R, Li R and Wang J 2017 *RSC Adv.* **7** 44239
[12] Qiu R, Zhang D and Wang P 2013 *Corros. Sci.* **66** 350
[13] Elvira K S, Casadevall i Solvas X, Wootton R C and deMello A J 2013 *Nat. Chem.* **5** 905
[14] Venancio-Marques A and Baigl D 2014 *Langmuir* **30** 4207
[15] Jiao Z Z, Zhou H, Han X C, Han D D and Zhang Y L 2023 *J. Colloid Interface Sci.* **629** 582
[16] Basu S, Hanh B M, Isaiah Chua J Q, Daniel D, Ismail M H, Marchioro M, Amini S, Rice S A and Miserez A 2020 *J. Colloid Interface Sci.* **568** 185
[17] Rowthu S and Hoffmann P 2018 *ACS Appl. Mater. Interfaces* **10** 10560
[18] Wang J, Kato K, Blois A P and Wong T S 2016 *ACS Appl. Mater. Interfaces* **8** 8265
[19] Wong T S, Kang S H, Tang S K Y, Smythe E J, Hatton B D, Grinthal A and Aizenberg J 2011 *Nature* **477** 443
[20] Hao C, Liu Y, Chen X, He Y, Li Q, Li K Y and Wang Z 2014 *Sci. Rep.* **4** 6846
[21] Fang Y, Liang J, Bai X, Yong J, Huo J, Yang Q, Hou X and Chen F 2020 *Langmuir* **36** 15403
[22] Wen T, Zhang C, Gong Y, Liu Z, Zhao W, Zhan Y, Zhang C, Wang K and Bai J 2023 *Polymers* **15** 1132
[23] Li Q, Wu D and Guo Z 2019 *Soft Matter* **15** 6803
[24] Qian C, Chen Z, Meng X, Li Q and Chen X 2023 *Chem. Eng. J.* **469** 143819
[25] Huang T, Zhang L, Lao J, Luo K, Liu X, Sui K, Gao J and Jiang L 2022 *ACS Appl. Mater. Interfaces* **14** 17968
[26] Makkonen L 2016 *J. Phys. Condens. Matter* **28** 135001
[27] Chaudhury M K and Whitesides G M 1992 *Science* **256** 1539
[28] Ricci E, Sangiorgi R and Passerone A 1986 *Surf. Coat. Technol.* **28** 215
[29] Wu S Z, Zhou L L, Chen C, Shi L A, Zhu S W, Zhang C C, Meng D, Huang Z C, Li J W, Hu Y L and Wu D 2019 *Langmuir* **35** 13915
[30] Zhao H, Wang D R, Zha J W, Zhao J and Dang Z M 2013 *J. Mater. Chem. A* **1** 3140
[31] Hwang H, Papadopoulos P, Fujii S and Wooh S 2022 *Adv. Funct. Mater.* **32** 2111311